

Supporting Information for
**Dust pollution in China affected by different spatial and
temporal types of El Niño**

Yang Yang^{1*#}, Liangying Zeng^{1#}, Hailong Wang², Pinya Wang¹, Hong Liao¹

¹Jiangsu Key Laboratory of Atmospheric Environment Monitoring and Pollution
Control, Jiangsu Collaborative Innovation Center of Atmospheric Environment and
Equipment Technology, School of Environmental Science and Engineering, Nanjing
University of Information Science and Technology, Nanjing, Jiangsu, China

²Atmospheric Sciences and Global Change Division, Pacific Northwest National
Laboratory, Richland, Washington, USA

Contents of this file

Figures S1 to S8

*Correspondence to yang.yang@nuist.edu.cn

These authors contributed equally to this work

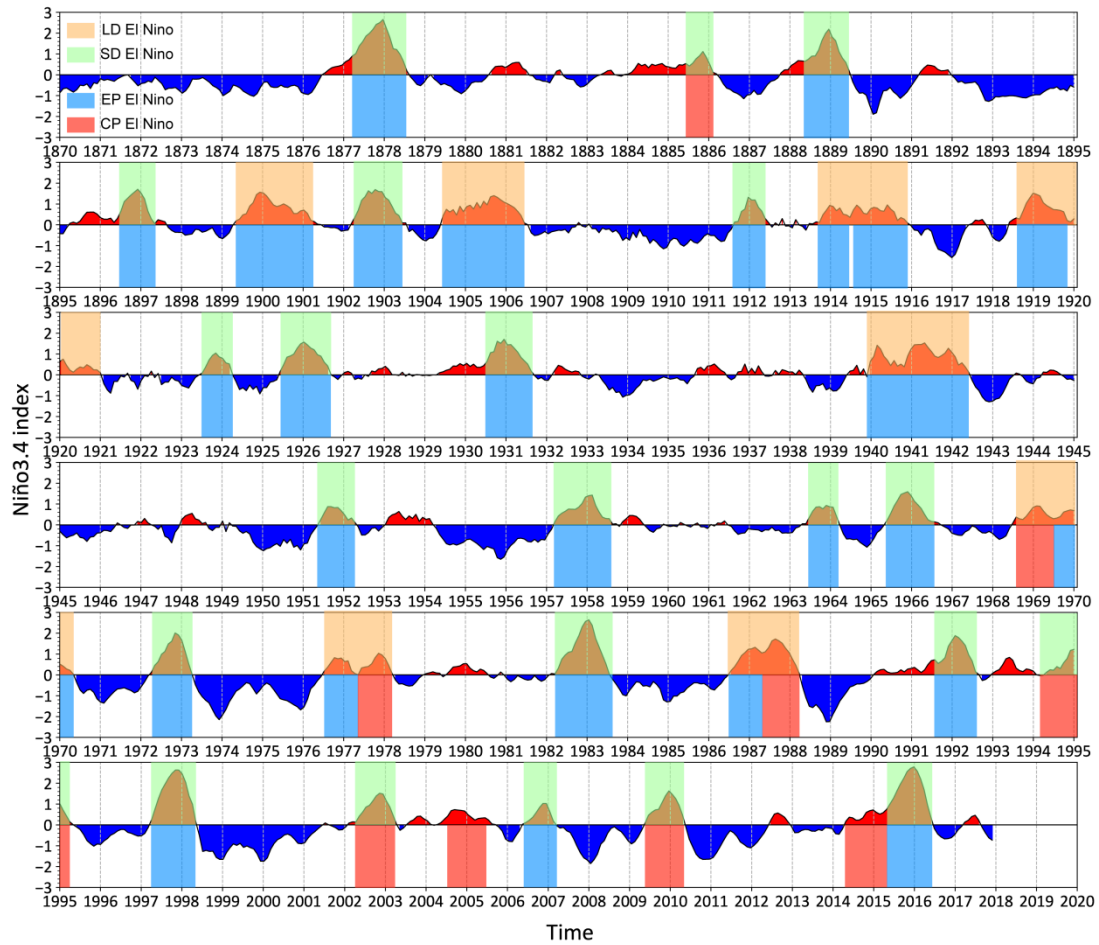


Figure S1. Time series of the Niño3.4 index ($^{\circ}\text{C}$) based on the merged Hadley-NOAA/OI SST dataset for 1870–2017. The time series were detrended and smoothed with a 3-month running average filter. Highlighted slots illustrate the EP (blue, 1877/1878, 1888/1889, 1896/1897, 1899/1900, 1902/1903, 1904/1905, 1911/1912, 1913/1914, 1914/1915, 1918/1919, 1923/1924, 1925/1926, 1930/1931, 1939/1940, 1951/1952, 1957/1958, 1963/1964, 1965/1966, 1972/1973, 1976/1977, 1982/1983, 1986/1987, 1991/1992, 1997/1998, 2006/2007), CP (red, 1885/1886, 1968/1969, 1977/1978, 1994/1995, 2002/2003, 2004/2005, 2009/2010, 2014/2015), SD (green, 1877/1878, 1885/1886, 1888/1889, 1896/1897, 1902/1903, 1911/1912, 1923/1924, 1925/1926, 1930/1931, 1951/1952, 1957/1958, 1963/1964, 1965/1966, 1972/1973, 1982/1983, 1991/1992, 1994/1995, 1997/1998, 2002/2003, 2006/2007, 2009/2010, 2015/2016) and LD (orange, 1899/1900, 1904/1905, 1913/1914, 1918/1919, 1939/1940, 1968/1969, 1976/1977, 1986/1987) El Niño events.

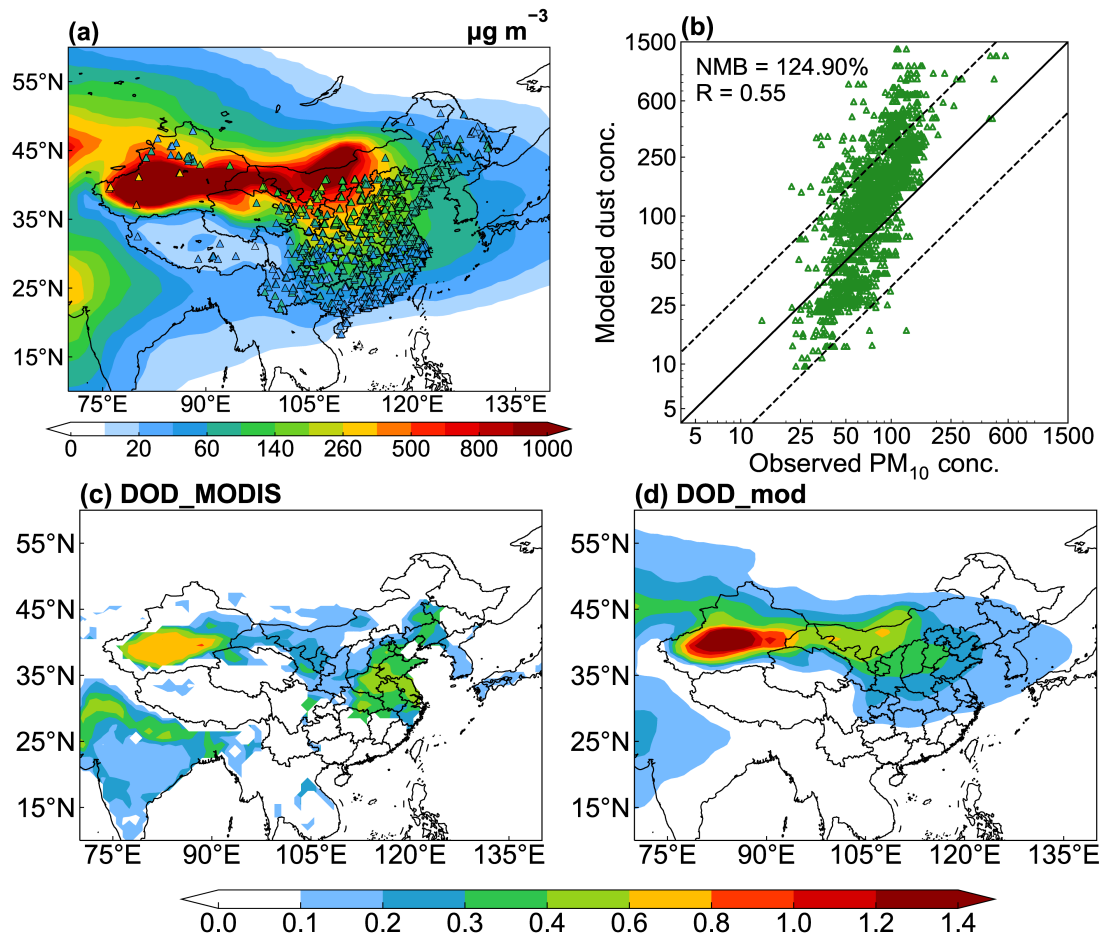


Figure S2. Spatial distributions (a) and scatter plots (b) of MAM mean observed near-surface PM₁₀ concentrations ($\mu\text{g m}^{-3}$, color-filled triangles in a) and simulated dust concentrations ($\mu\text{g m}^{-3}$, contour in a) from the CLIM experiment. Solid line represents 1:1 ratio and dashed lines mark 1:3 and 3:1 ratios. The observed concentrations are derived from the CNEMC in 2015–2021. The normalized mean deviation (NMB) and the correlation coefficient (R) between observations and simulation are shown in the upper left corner of (b). $\text{NMB} = 100\% \times \frac{\sum (M_i - O_i)}{\sum O_i}$, where M_i and O_i are the simulated and observed values at the site i , respectively. Spatial distributions of MAM mean Dust Aerosol Optical Depth (DOD) from MODIS over 2001–2020 and CLIM experiment are shown in (c) and (d), respectively.

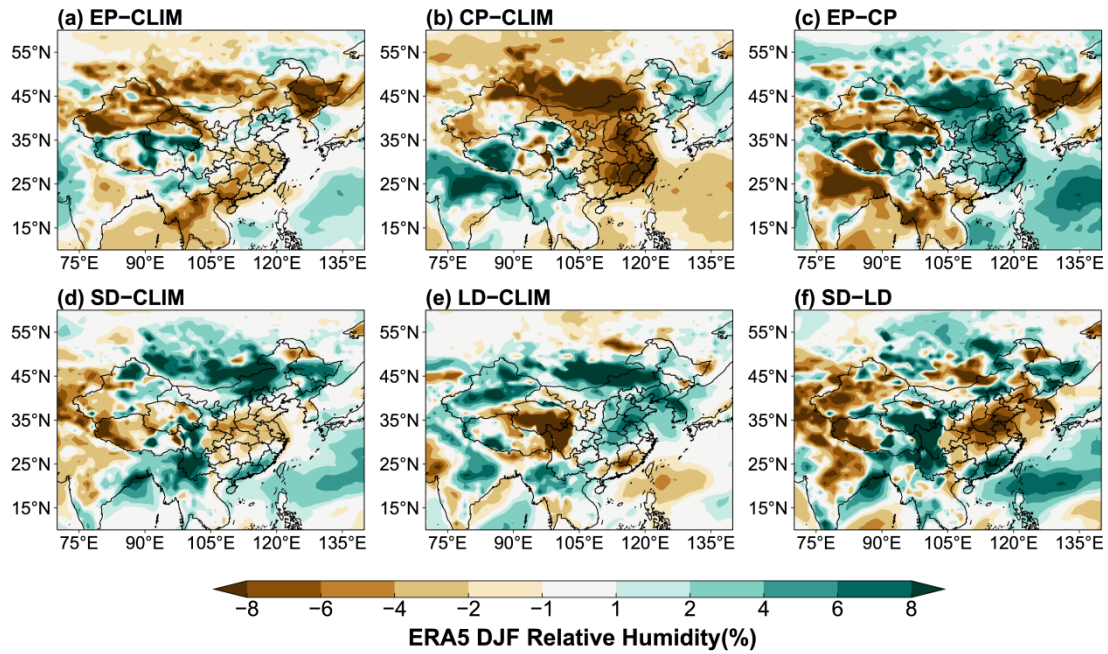


Figure S3. Composite differences in DJF mean relative humidity (units: %) between 2006/07 EP El Niño and climatological mean (1950–2017) in (a), 2014/15 CP El Niño and climatological mean in (b), 2006/07 EP El Niño and 2014/15 CP El Niño in (c), 2015/16 SD El Niño and climatological mean in (d), 1986/87 LD El Niño and climatological mean in (e), 2015/16 SD El Niño and 1986/87 LD El Niño in (f) from the ERA5 reanalysis data. The data were detrended over 1950–2017.

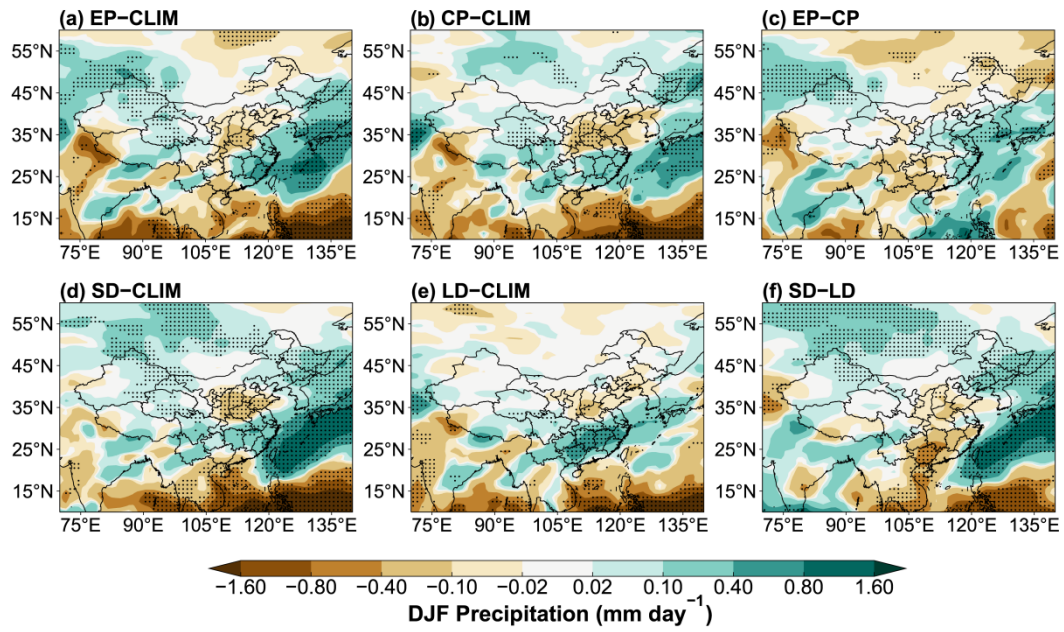


Figure S4. Composite differences in DJF mean precipitation (mm day^{-1}) between EP and CLIM in (a), CP and CLIM in (b), EP and CP in (c), SD and CLIM in (d), LD and CLIM in (e), and SD and LD in (f). The stippled areas indicate statistical significance with 90% confidence from a two-tailed T-test.

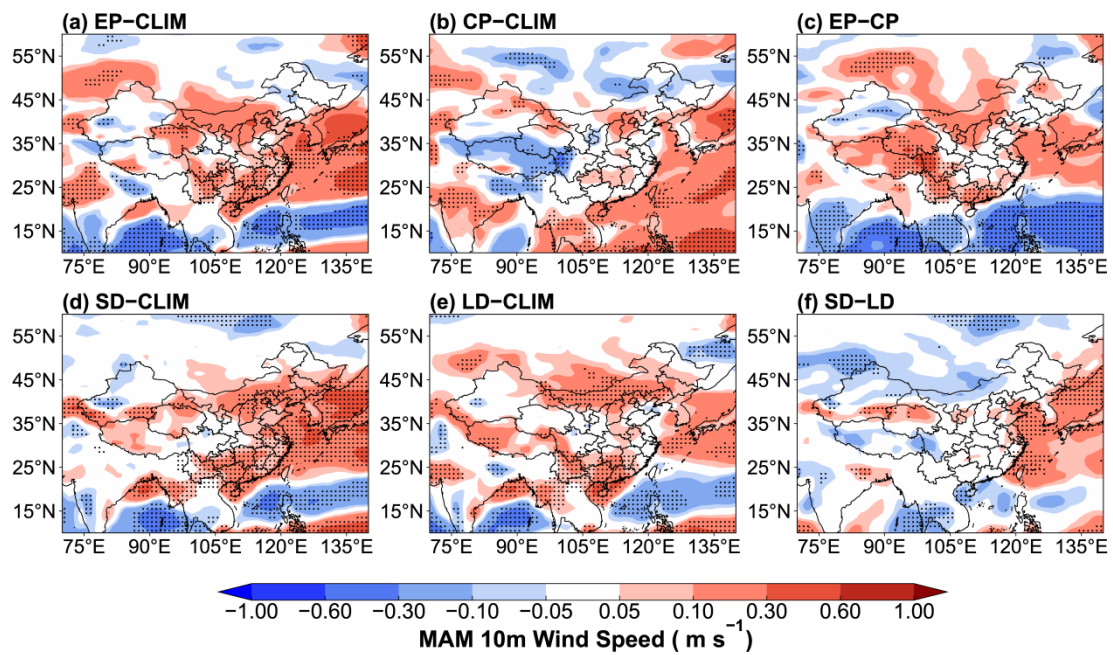


Figure S5. Composite differences in MAM mean 10-m wind speed (m s^{-1}) between EP and CLIM in (a), CP and CLIM in (b), EP and CP in (c), SD and CLIM in (d), LD and CLIM in (e), and SD and LD in (f). The stippled areas indicate statistical significance with 90% confidence from a two-tailed T-test.

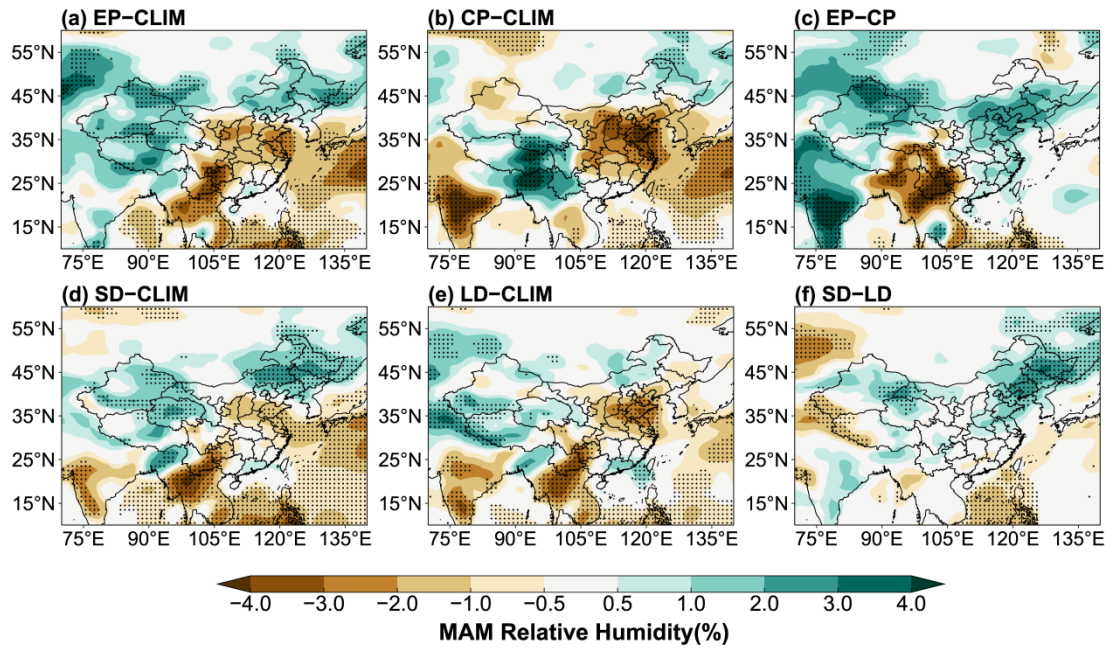


Figure S6. Composite differences in MAM mean relative humidity (units: %) between EP and CLIM in (a), CP and CLIM in (b), and EP and CP in (c), SD and CLIM in (d), LD and CLIM in (e), and SD and LD in (f). The stippled areas indicate statistical significance with 90% confidence from a two-tailed T-test.

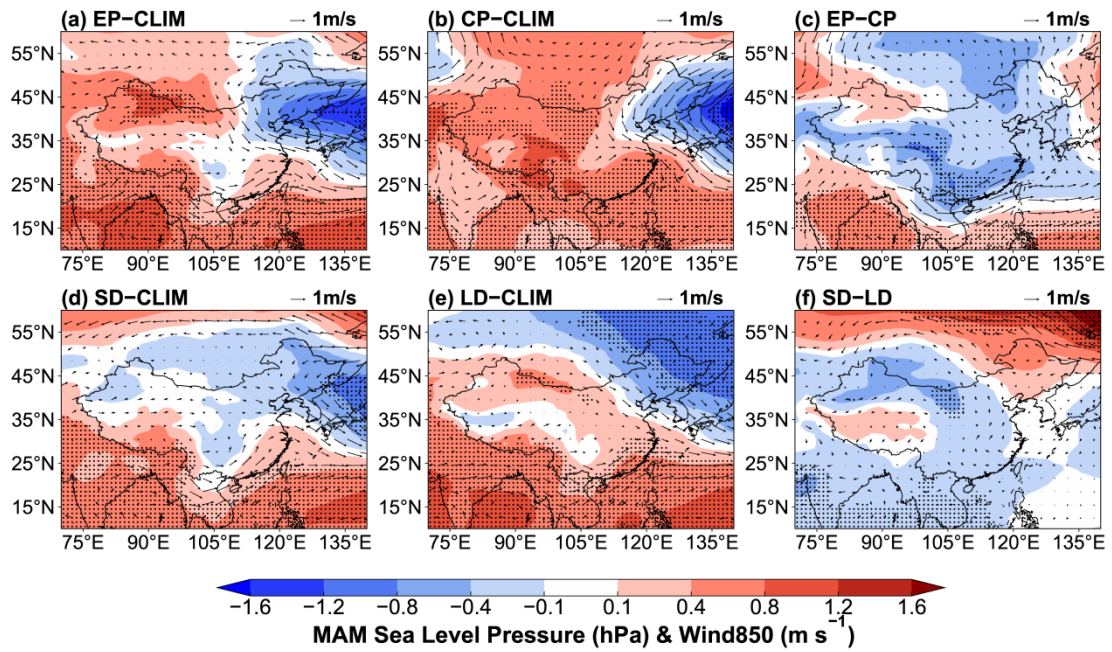


Figure S7. Composite differences in MAM mean sea level pressure (SLP, shaded; units: hPa) and wind at 850 hPa (WIND850, vector; units: m s^{-1}) between EP and CLIM in (a), CP and CLIM in (b), and EP and CP in (c), SD and CLIM in (d), LD and CLIM in (e), and SD and LD in (f). The stippled areas indicate statistical significance with 90% confidence from a two-tailed T-test.

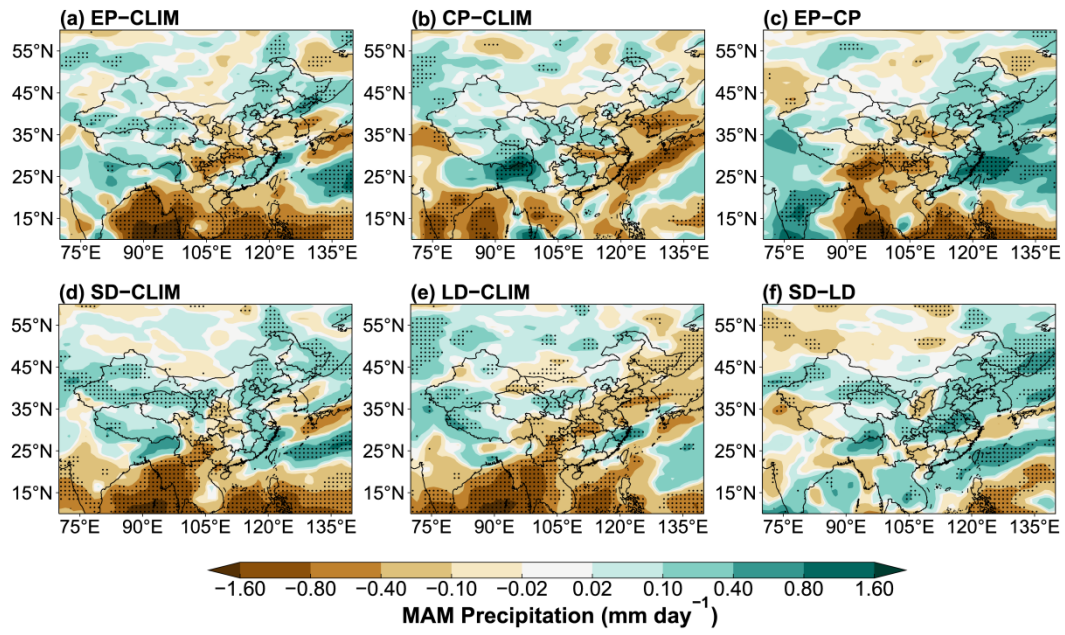


Figure S8. Composite differences in MAM mean precipitation (mm day^{-1}) between EP and CLIM in (a), CP and CLIM in (b), EP and CP in (c), SD and CLIM in (d), LD and CLIM in (e), and SD and LD in (f). The stippled areas indicate statistical significance with 90% confidence from a two-tailed T-test.